Natural convection in vertical channels with an auxiliary plate

Assunta Andreozzi and Oronzio Manca
Dipartimento di Ingegneria Aerospaziale e Meccanica, Seconda Università degli Studi di Napoli, Real Casa dell'Annunziata, Aversa (CE), Italy

Vincenzo Naso
Dipartimento di Energetica, Termofluidodinamica applicata e Condizionamenti ambientali, Università degli Studi di Napoli Federico II, Napoli, Italy

Keywords *Natural convection, Numerical simulation, Electronics, Cooling*

Abstract *Research on natural convection in open channels is very extensive due to its role in many engineering applications such as thermal control of electronic systems. In this paper, a parametric analysis is carried out in order to add knowledge of heat transfer in air natural convection for a symmetrically heated vertical parallel plate channel with a central auxiliary heated or adiabatic plate. The two-dimensional steady-state problem is solved by means of the stream function–vorticity approach and the numerical solution is carried out by means of the control volume method. Results are obtained for both a heated and unheated auxiliary plate, for a Rayleigh number in the range 10^3–10^6, for a ratio of the auxiliary plate height to the channel plate height equal to 0, 0.5 and 1 and for a ratio of the channel length to the channel gap in the range 5–15. Correlations for maximum wall temperatures and average channel Nusselt numbers are proposed.*

Nomenclature

a = thermal diffusivity, m^2/s
b = channel gap, m
g = gravity acceleration, m/s^2
Gr = Grashof number, equation (5)
h = auxiliary plate height, m
h_x = local convective coefficient, $W/m^2 K$
k = thermal conductivity, W/m K
L = channel plate height, m
L_x = height of the reservoir, m
L_y = width of the reservoir, m
Nu_x = local Nusselt number, equations (9) and (10)
Nu = average Nusselt number, equations (11) and (12)
p = pressure, Pa
P = dimensionless pressure, equation (5)
Pr = Prandtl number, equation (5)
$\dot{q}$ = heat flux, W/m^2
Ra = Rayleigh number, equation (5)
Ra* = channel Rayleigh number, equation (5)
t = time, s
T = temperature, K
u, v = velocity components along x, y, m/s
U, V = dimensionless velocities, equation (5)

International Journal of Numerical Methods for Heat & Fluid Flow, Vol. 12 No. 6, 2002, pp. 716-734.

DOI 10.1108/09615530210438364

This research is funded by the MIUR under the 2001 grant for the research program:" *Single phase natural and mixed convection: fundamentals and applications in thermal systems and components*".

x_q = heat flux ratio, equation (5)
x, y = cartesian coordinates, m
X, Y = dimensionless coordinates

Greek

β = volumetric coefficient of expansion, 1/K
Δ = difference between two values
ϵ = convergence criterion
η = dummy variable
θ = dimensionless temperature, equation (5)
μ = dynamic viscosity, kg/(ms)
ν = kinematic viscosity, m^2/s
ψ = stream function, m^2/s
Ψ = dimensionless stream function, equation (5)
ρ = density, kg/m^3
ω = vorticity, 1/s
Ω = dimensionless vorticity, equation (5)
Φ = dissipation function, $1/s^2$

Subscripts

∞ = free-stream condition
max = maximum value
w_1 = channel wall
w_2 = center line
p = auxiliary plate
0 = refers to the channel without auxiliary plate ("base case")

Introduction

Natural convection is very attractive since it is cheap, reliable, quiet and maintenance free (Peterson and Ortega, 1990). Due to its role in many engineering applications, such as thermal control of electronic systems, solar installations and heat exchangers, extensive research on natural convection in open channels has been carried out by Peterson and Ortega (1990); Raithby and Hollands (1998); Manca *et al.* (2000); Bianco *et al.* (2000). In recent years, trends in the thermal design of natural convection between parallel plates for electronic systems cooling are: the optimization of simple configurations and the design of configurations derived from the simple channel, both of which could improve heat transfer (Bar-Cohen and Rohsenow, 1984; Bejan, 1984; Peterson and Ortega, 1990; Kin and Lee, 1996; Bar-Cohen and Kraus, 1998; Ledezma and Bejan, 1997; Morrone *et al.*, 1997; Manca and Nardini, 2001). A good knowledge of the thermal and geometrical parameters and of their influence on the system's thermal performance requires the investigation of the physical behavior of the system. In this way, it is possible to define the thermal design procedure and obtain optimized configurations. This process can be achieved by means of the parametric analysis of the numerical solution to the problem.

The configuration of vertical parallel plate channel with an auxiliary plate in the centerline of the channel has scarcely been studied. As reported in Aihara *et al.* (1996), this configuration was introduced by Aihara (1963). Cheng *et al.* (1988) investigated a channel with isothermal walls with an auxiliary plate, either isothermal or isoflux. The numerical solution was carried out with boundary layer approximation and taking into account the pressure drop at the channel inlet. Results were obtained for channel Rayleigh numbers in the range 10^{-1}–10^2 and with dimensionless heights of the auxiliary plate in the range 0.005–0.7. The temperature difference ratios were chosen to be 0.001, 0.5 and 1 for isothermal central plates and the dimensionless heat flux was equal to 0, 1 and 5 for an isoflux auxiliary plate. A similar numerical approach was adopted

in Aihara *et al.* (1996) for a vertical parallel plate channel with isothermal walls and an isothermal auxiliary central plate. The auxiliary plate was placed in three different locations and it was found that the best position was in the inlet region. Results were given for channel Rayleigh numbers less than 10^4, for dimensionless heights of the auxiliary plate in the 0.0–1.0 range. Numerical solutions of the fully elliptic approach and parabolic form of the governing equations were carried out in Naylor and Tarasuk (1993a), for the same problem given in Aihara *et al.* (1996). The Navier–Stokes and energy equations were solved using the finite element code FIDAP, with the inlet channel conditions based on a Jeffrey–Hamel flow in an upward reservoir. A forward marching finite difference procedure was used to solve the parabolic problem. The authors found the fully developed solution for $Ra^* \rightarrow 0$ and they gave results for different positions of the auxiliary plate; channel Rayleigh number and dimensionless auxiliary plate height ranged between $5–10^4$ and 0.0–1.0, respectively, while the aspect ratio was equal to 15. They also took into account the effects of the plate thickness. In Naylor and Tarasuk (1993b) the same authors carried out an experimental study by means of a Mach–Zehender interferometer on the same configuration given in Naylor and Tarasuk (1993a). The auxiliary pla te was located either at the bottom or at the top of the channel and its dimensionless height was 1/3. Experimental and numerical results were in good agreement even if the experimentally measured average Nusselt numbers were about 10 percent lower than the numerical ones. Correlations for the average Nusselt numbers were proposed. Multiple vertical isothermal parallel plate channels were numerically investigated in Floryan and Novak (1994) by using the FIDAP code. Results for two parallel channels (dimensionless height of the auxiliary plate equal to 1.0) were obtained for Grashof channel numbers between 5.0×10^2 and 2.0×10^4 and the effect of the auxiliary plate was analyzed. The symmetrically heated configuration with walls at uniform heat flux was analyzed in Andreozzi *et al.* (1999) and Andreozzi and Manca (2001) the same arrangement with adiabatic extensions downstream of the channel walls was investigated by Andreozzi *et al.* (2000). The fully elliptic problem was numerically solved by means of a finite volume method and the computational domain consisted of the channel and two reservoirs located upstream and downstream of the channel. In Andreozzi *et al.* (1999) and in Andreozzi and Manca (2001), results were given for air; channel Rayleigh numbers and dimensionless auxiliary plate heights ranged between $10^3–10^6$ and 0.0–1.0, respectively, and the channel aspect ratio was equal to 10. In Andreozzi and Manca (2001), two correlations for average channel Nusselt numbers were proposed, one for an adiabatic auxiliary plate and the other for a heated auxiliary plate. The ranges of channel Rayleigh numbers and of auxiliary plate heights were $10^2–10^5$ and 0.0–1.0, respectively. In Andreozzi *et al.* (2000), results were given for aspect ratios less than 1.5 and for channel Rayleigh numbers equal to 2.1×10^2 and 5.7×10^6.

For the configuration analyzed in Andreozzi *et al.* (1999, 2000), there is a lack of research on the effect of the channel aspect ratio on the thermal behavior of the channel. In this paper, a parametric analysis is carried out to add knowledge on air natural convection in an isoflux symmetrically heated vertical parallel plate channel with a central auxiliary heated or adiabatic plate; the auxiliary plate is located in the inlet region of the channel. The numerical solution to the fully elliptic problem is obtained by means of a finite volume method on a I-shaped computational domain (Andreozzi *et al.*, 1999; 2000). Results are given in terms of dimensionless wall temperature, mass flow rate, maximum wall temperature and average channel Nusselt number. Results are obtained for air, heated and unheated auxiliary plate, Rayleigh numbers in the range 10^3–10^6, auxiliary plate heights equal to 0, 0.5 and 1 and channel aspect ratios in the range 5–15. The above-mentioned ranges are those typically used in common applications, such as electronics cooling. Correlations for maximum wall temperatures and average channel Nusselt numbers are proposed.

Analysis and numerical solution method

The configuration of the problem studied in this paper is shown in Figure 1(a). It is composed of a vertical parallel plate channel with a very thin auxiliary plate placed in its mid-plane. The basic geometry is characterized by the height of the channel plates L, the channel gap b and the height of the auxiliary plate h, which varies between 0 and L. The parallel plates are heated with a uniform heat flux equal to $\dot{q}$, while the auxiliary plate can be either insulated or heated with a uniform heat flux, $\dot{q}_{\mathrm{p}}$. Consequently, the main ratios employed in the analysis are: L/b, the ratio of the channel height to the channel gap (aspect ratio), h/L, the ratio of the auxiliary plate height to the channel height, and the ratio of the auxiliary plate heat flux to the parallel plate channel one, $x_q = \dot{q}_{\mathrm{p}}/\dot{q}$, which can be 0 or 1.

By defining the stream function and vorticity as

$$\frac{\partial \psi}{\partial y} = u; \qquad \frac{\partial \psi}{\partial x} = -v; \qquad \omega = \frac{\partial v}{\partial x} - \frac{\partial u}{\partial y} \tag{1}$$

the transformed governing equations, for the two-dimensional problem and steady-state regime, can be written in the following way:

$$\frac{\partial (u\omega)}{\partial x} + \frac{\partial (v\omega)}{\partial y} = \nu \nabla^2 \omega - g\beta \frac{\partial T}{\partial y} \tag{2}$$

$$\frac{\partial^2 \psi}{\partial x^2} + \frac{\partial^2 \psi}{\partial y^2} = -\omega \tag{3}$$

$$\frac{\partial (uT)}{\partial x} + \frac{\partial (vT)}{\partial y} = a \nabla^2 T + \mu \Phi + T\beta \frac{Dp}{Dt} \tag{4}$$

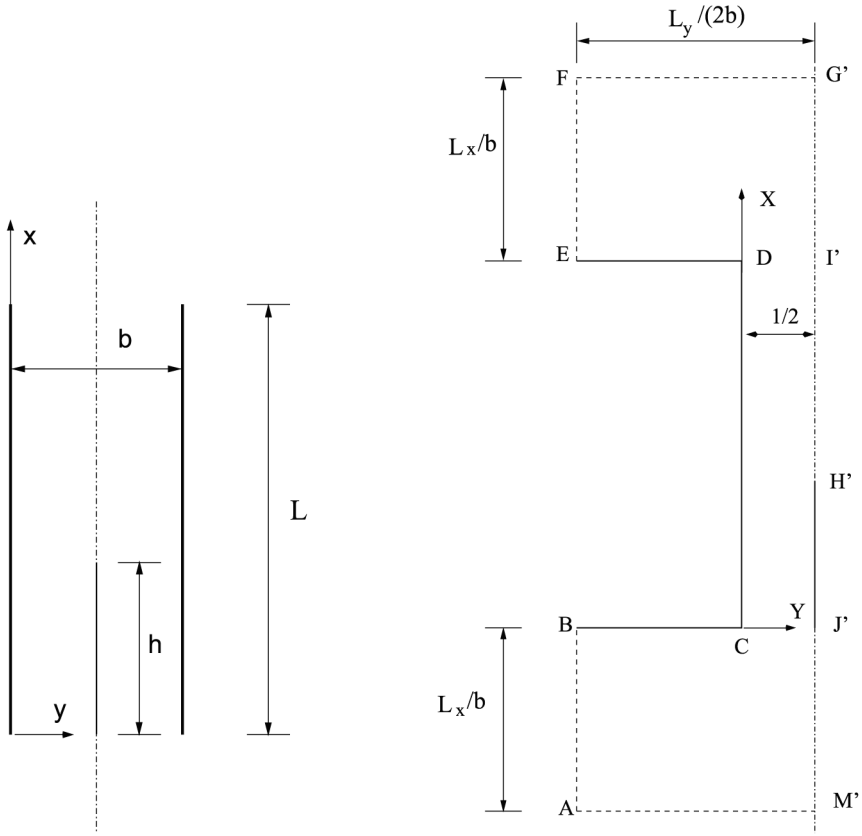

(a) Physical domain **(b)** Computational domain

Figure 1.
Geometry of the problem

In equation (4), the terms of dissipation and total derivative of pressure were neglected, since in natural convection temperature gradients are generally weak (Gebhart *et al.*, 1988). Moreover, the thermophysical properties were assumed to be independent of the temperature, except for the density, as suggested by the Boussinesq approximation.

The following dimensionless variables are defined:

$$X = \frac{x}{b}, \qquad Y = \frac{y}{b}, \qquad U = \frac{ub}{\nu}, \qquad V = \frac{vb}{\nu}, \qquad P = \frac{(p - p_\infty)b^2}{\rho\,\nu^2}$$

$$\theta = \frac{(T - T_\infty)k}{\dot{q}\,b}, \qquad \Psi = \frac{\psi}{\nu}, \qquad \Omega = \frac{\omega b^2}{\nu}$$

$$\mathrm{Gr} = \frac{g\,\beta\,\dot{q}\,b^4}{k\,\nu^2}, \qquad \mathrm{Pr} = \frac{\nu}{a}, \qquad \mathrm{Ra} = \mathrm{Gr}\,\mathrm{Pr}, \qquad \mathrm{Ra}^* = \mathrm{Ra}\frac{b}{L}, \qquad x_q = \frac{\dot{q}_p}{\dot{q}} \quad (5)$$

The dimensionless form of the equations (2)–(4) is:

$$\frac{\partial(U\Omega)}{\partial X}+\frac{\partial(V\Omega)}{\partial Y}=\nabla^2\Omega-\mathrm{Gr}\frac{\partial\theta}{\partial Y} \tag{6}$$

$$\frac{\partial^2\Psi}{\partial X^2}-\frac{\partial^2\Psi}{\partial Y^2}=-\Omega \tag{7}$$

$$\frac{\partial(U\theta)}{\partial X}+\frac{\partial(V\theta)}{\partial Y}=\frac{1}{\mathrm{Pr}}\nabla^2\theta \tag{8}$$

From the numerical point of view, an enlarged computational domain was chosen to mimic the free-stream conditions. It is composed of the channel with an auxiliary plate and two reservoirs of height L_x and width L_y, which are placed upstream and downstream of the channel. Due to thermofluidynamic and geometrical symmetries, the problem is solved in half the domain, as shown in Figure 1(b). With reference to Figure 1(b), the imposed boundary conditions are reported in Table I.

The local convective heat transfer over the channel plate is described by the local Nusselt number, defined as

$$\mathrm{Nu}_x=\frac{h_x\,b}{k}=\frac{1}{\theta_{w1}(x)} \tag{9}$$

while the local Nusselt number over the auxiliary plate, when $x_q \neq 0$, is:

$$\mathrm{Nu}_{x\mathrm{p}}=\frac{h_{x\mathrm{p}}\,b}{k}=\frac{x_q}{\theta_{\mathrm{p}}(x)} \tag{10}$$

Ψ	Ω	θ	Zone
$\frac{\partial^2\Psi}{\partial Y^2}=0$	$\frac{\partial\Omega}{\partial Y}=0$	$\theta=0$	AB
$\frac{\partial^2\Psi}{\partial X^2}=0$	$\frac{\partial\Omega}{\partial X}=0$	$\theta=0$	AM′
$\Psi=\Psi_{\mathrm{w1}}$	$\frac{\partial\Psi}{\partial X}=0$	$\frac{\partial\theta}{\partial X}=0$	BC and DE
$\Psi=\Psi_{\mathrm{w1}}$	$\frac{\partial\Psi}{\partial Y}=0$	$\frac{\partial\theta}{\partial Y}=-1$	CD
$\Psi=\Psi_{\mathrm{w2}}$	$\frac{\partial\Psi}{\partial Y}=0$	$\frac{\partial\theta}{\partial Y}=x_q$	J′H′
$\frac{\partial^2\Psi}{\partial Y^2}=0$	$\frac{\partial\Omega}{\partial Y}=0$	$\frac{\partial\theta}{\partial Y}=0$	EF
$\Psi=\Psi_{\mathrm{w2}}$	$\Omega=0$	$\frac{\partial\theta}{\partial Y}=0$	H′G′ and M′J′
$\frac{\partial^2\Psi}{\partial X^2}=0$	$\frac{\partial\Omega}{\partial X}=0$	$\frac{\partial\theta}{\partial X}=0$	FG′

Table I. Boundary conditions

The corresponding average values can be written as:

$$\mathrm{Nu} = \frac{b}{L}\int_0^{L/b} \mathrm{Nu}_x \; \mathrm{d}X \tag{11}$$

$$\mathrm{Nu}_\mathrm{p} = \frac{b}{h}\int_0^{h/b} \mathrm{Nu}_{x\mathrm{p}} \; \mathrm{d}X \tag{12}$$

The numerical solution to equations (6)–(8) is carried out by employing the control volume method and for $\mathrm{Pr} = 0.71$. In the problem under investigation, the induced mass flow rate is an unknown function of the thermo-geometrical parameters such as L/b, h/L and the Rayleigh number. Consequently, the stream function values on the channel plate, Ψ_{w1}, and on the centerline, Ψ_{w2}, are not known in advance, since $\Delta\Psi = \Psi_{w2} - \Psi_{w1}$ represents the induced volumetric flow rate in half the channel. Thereafter, the $\Delta\Psi$ value should be guessed at first. Then, through an iterative procedure, the correct value of this unknown quantity must be determined. The iterative procedure is the following:

(1) assign a guessed $\Delta\Psi$ value;

(2) solve equations (6)–(8), using the Alternating Direction Implicit; technique (ADI);

(3) solve the stream function equation (7) by the SLOR method with an optimal value of the relaxation factor of about 1.7;

(4) once equations (6)–(8) have been solved, the following convergence criteria for the time-like step

$$\left|\frac{\eta_{ij}^{n+1} - \eta_{ij}^{n}}{\eta_{ij}^{n+1}}\right|_{\max} < \epsilon \tag{13}$$

has to be verified, where η represents either Ω or θ and the 10^{-5} common value is assumed for ϵ;

(5) once the steady-state is attained, the guessed induced mass flow rate is checked. The selected value of the mass flow rate is checked by integrating the momentum equation along the centerline of the channel in the chosen computational domain. The following condition must occur:

$$\int_{-L_x/b}^{(L_x+L)/b} \frac{\partial P}{\partial X}\,\mathrm{d}X = 0 \tag{14}$$

If this equation is not satisfied within a prescribed accuracy (10^{-2}), return to step 1 and repeat the whole procedure until a converged solution is obtained.

Tests on the relaxation factor evaluation have been made and they have given as result an optimum value equal to 1.7. As far as the sensitivity of the grid is concerned, it depends on two major components: the mesh spacing and the dimensions of the upstream and downstream reservoirs. After testing several combinations of nodes in the grid, a uniform 51×27 mesh for the channel region was chosen because it ensured a good compromise between the machine computational time and the accuracy requirements. In fact, by increasing the number of nodes along Y from 13 to 27, the induced mass flow rate, $\Delta\Psi$, and the average Nusselt number, Nu, show a variation of about 1.5 percent and the same variables exhibit a weaker dependence on the number of nodes along X. Moreover other tests have been made by employing the Richardson extrapolation (Roache, 1998) and the percentage discrepancies between the overall variables, $\Delta\Psi$ and Nu, and the corresponding asymptotic values were less than 1 percent. Depending on the Rayleigh number value, a reservoir vertical dimension, L_x, two times the channel height and a reservoir horizontal width, L_y, 21 times the channel gap, b, were chosen. This procedure was successfully tested by comparing its results with other numerical and experimental outcomes (Manca *et al.*, 1994).

Results and discussion

A parametric analysis on air ($\mathrm{Pr} = 0.71$) natural convection in a symmetrically heated vertical channel with an auxiliary plate, in terms of wall temperatures, maximum wall temperature, dimensionless mass flow rates and average Nusselt numbers, was carried out.

Results are given for a heated and an unheated auxiliary plate, for Rayleigh numbers in the range 10^3–10^6, for auxiliary plate heights equal to 0, 0.5 and 1.0, for channel aspect ratios in the range 5–15.

Wall temperature profiles as a function of the vertical coordinate for the configurations with the auxiliary plate unheated ($x_q = 0.0$), $h/L = 0.5$ and 1.0, $\mathrm{Ra} = 10^3$ and 10^6 and $L/b = 5$, 10 and 15 are shown in Figure 2.

In Figures 2(a–c), a marked reduction in the channel wall temperature is observed at the channel outlet because of the edge effects due to the axial diffusion of heat which shifts the maximum wall temperature abscissa from the channel outlet towards the channel interior. The reduction is less marked at $\mathrm{Ra} = 10^6$ (Figures 2(d–f)). At $\mathrm{Ra} = 10^3$, the diffusive effects cause the auxiliary plate heating from the channel inlet whereas, for $\mathrm{Ra} = 10^6$, the auxiliary plate is practically unheated. When $\mathrm{Ra} = 10^3$, the channel wall temperature profile and the auxiliary plate temperature profile are nearly parallel in the developing flow region, next to the motion development region. On the contrary, for $X \geq h/L$ the slope of channel wall temperature profile increases until it returns to the initial slope. This is due to the development of the flow close to the auxiliary plate. For both Rayleigh number values, the dimensionless wall temperature increases when h/L increases; this could

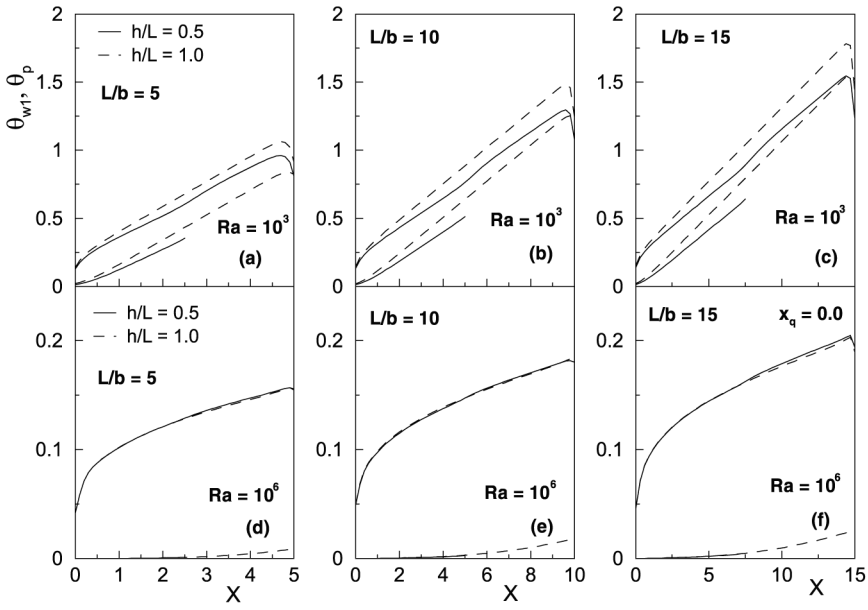

Note: (a), (b), (c) *Ra* = 10^3; **(d), (e), (f)** *Ra* = 10^6

Figure 2.
Wall temperature profiles vs the vertical coordinate for different h/L and L/b and $x_q = 0.0$: (a), (b), (c) Ra = 10^3; (d), (e), (f) Ra = 10^6

indicate a worsening chimney effect. In dimensional terms, however, it is noticeable that the wall temperature "decreases" as L/b increases, and the larger the Rayleigh number the greater this effect.

Wall temperature profiles as a function of the vertical coordinate for the configurations with $h/L = 0.5$ and 1.0, at Ra = 10^3 and 10^6 and for $L/b = 5, 10$ and 15, when the auxiliary plate is heated with a heat flux equal to that at the channel walls ($x_q = 1.0$), are shown in Figure 3.

Figure 3 shows that at the lowest Rayleigh number value the dimensionless temperatures of the channel wall and that of the auxiliary plate are nearly equal. Small differences in wall temperature profiles are determined by edge effects. Observing Figures 3(d–f), it can be remarked that at Ra = 10^6, which is pertinent to a Ohmic heat flux at the walls 1000 times that one for Ra = 10^3, at the same other dimensional parameters, the dimensional temperatures are 100 times than those at Ra = 10^3. It means also a significant improvement of the coefficient heat removal, which is determined by a stronger chimney effect in the system. Though the heat flux released to the fluid by the channel walls and by the auxiliary plate is the same, the temperature of the auxiliary plate is lower than that of the channel walls because the streamlines are stuck to it.

The maximum wall temperature, $\theta_{w1,\max}$, as a function of Rayleigh number, Ra, with $h/L = 0.0$, 0.5 and 1.0, $L/b = 10$, $x_q = 0.0$ and 1.0, is shown in Figure 4

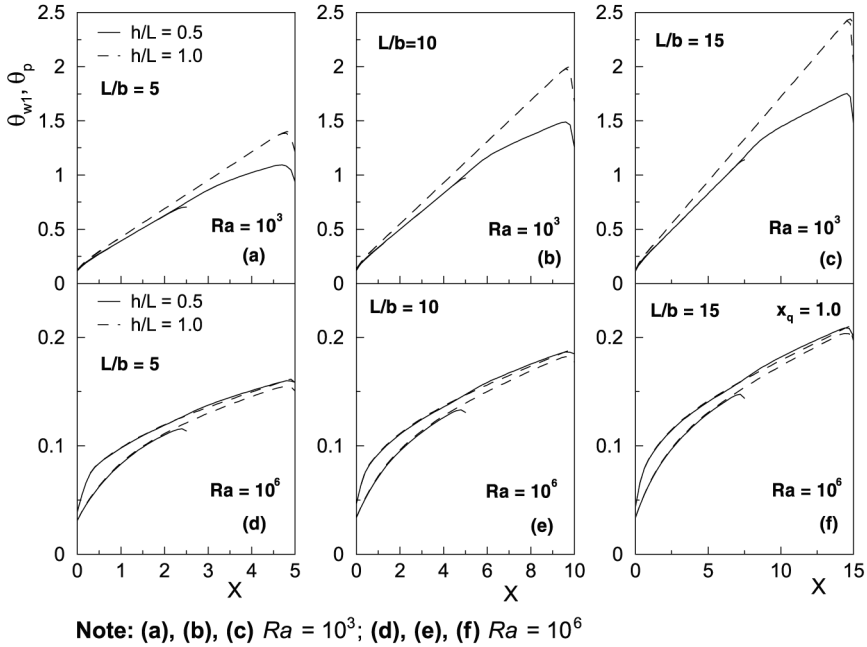

Figure 3.
Wall temperature profiles vs the vertical coordinate for different h/L and L/b and $x_q = 1.0$: (a), (b), (c) Ra $= 10^3$; (d), (e), (f) Ra $= 10^6$

It can be observed that the larger h/L the larger the maximum wall temperature both for $x_q = 0.0$ (Figure 4(a)) and for $x_q = 1.0$ (Figure 4(b)), because of the decrease in the "chimney effect" due to the larger pressure drop determined by the insertion of the auxiliary plate. It can also be noticed that, at increasing Rayleigh numbers, the increase in the maximum wall temperature is smaller. The increase in Rayleigh number is determined by the increase either in the channel gap or in the heat flux. This allows an improvement in the "chimney effect" and, consequently, an increase in the mass flow rate and in the heat transfer rate. Moreover, all analyzed configurations, at fixed x_q and L/b, show that maximum wall temperature curves tend to an asymptotic value and it is plain that $\theta_{w1,\max}$ values are practically equal when h/L refers to Rayleigh number larger than 10^5. Maximum wall temperatures are lower at $x_q = 0.0$ than at $x_q = 1.0$.

Dimensionless mass flow rate as a function of Rayleigh number, for the configurations with $L/b = 5$, 10 and 15 and with $h/L = 0.0$, 0.5 and 1.0 is shown in Figures 5 and 6, for $x_q = 0.0$ and 1.0, respectively.

Figure 5 ($x_q = 0.0$) shows that, as it was to be expected, the larger the Rayleigh number the larger the mass flow rate. This also occurs when L/b increases and it can seem contradictory. In fact, an increasing L/b means a decrease of b for a constant value of L and, therefore, an increase in the pressure loss. But, if the Rayleigh number is constant, there is a marked heat transfer

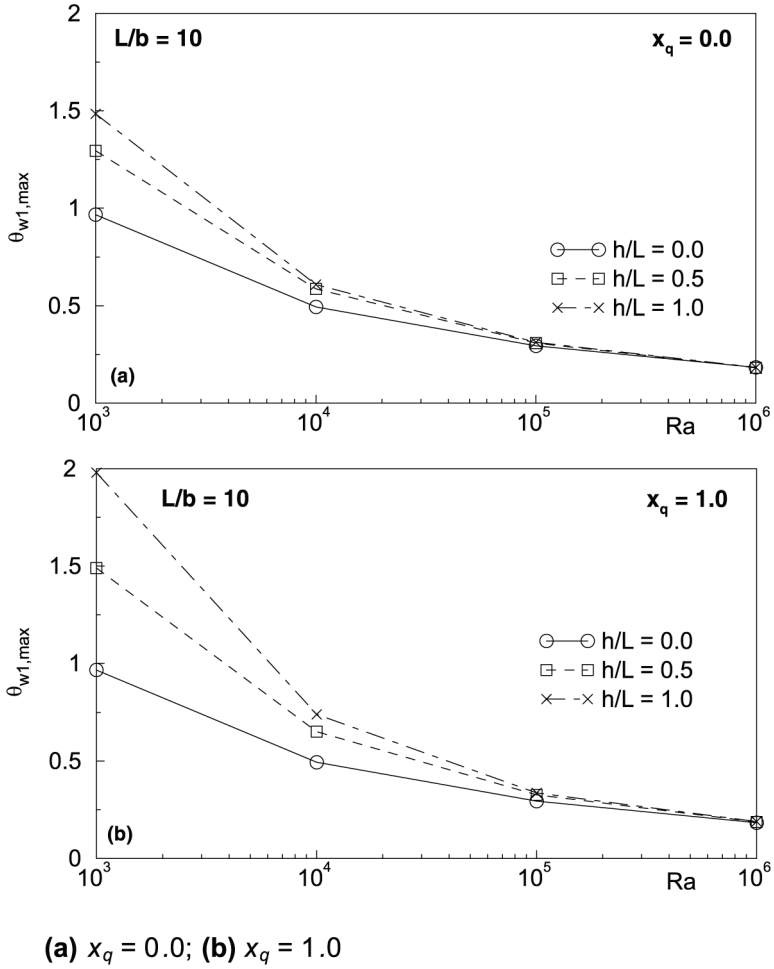

Figure 4.
Maximum wall temperature vs Rayleigh number for different h/L and $L/b = 10$: (a) $x_q = 0.0$; (b) $x_q = 1.0$

increase, that is a strong driving force increase. At the largest Ra (10^6), increasing L/b determines a larger increase in the mass flow than the one at the lowest Ra (10^3). Moreover, the mass flow rate decreases as h/L increases because of the increase in the pressure loss. The larger L/b the larger the difference between the configuration without the auxiliary plate ($h/L = 0.0$) and the configuration with an unheated auxiliary plate, particularly at the largest investigated Ra (10^6). The mass flow rate, $\Delta\Psi$, increases as Ra and L/b increase also for the configuration with $x_q = 1.0$ (see Figure 6). In fact, the increase in the mass flow rate occurs in this case too, but the heated auxiliary plate determines a larger mass flow rate increase at Ra $\geq 10^5$, independently of L/b. When Ra is lower than 10^4, the channel with the auxiliary plate exhibits

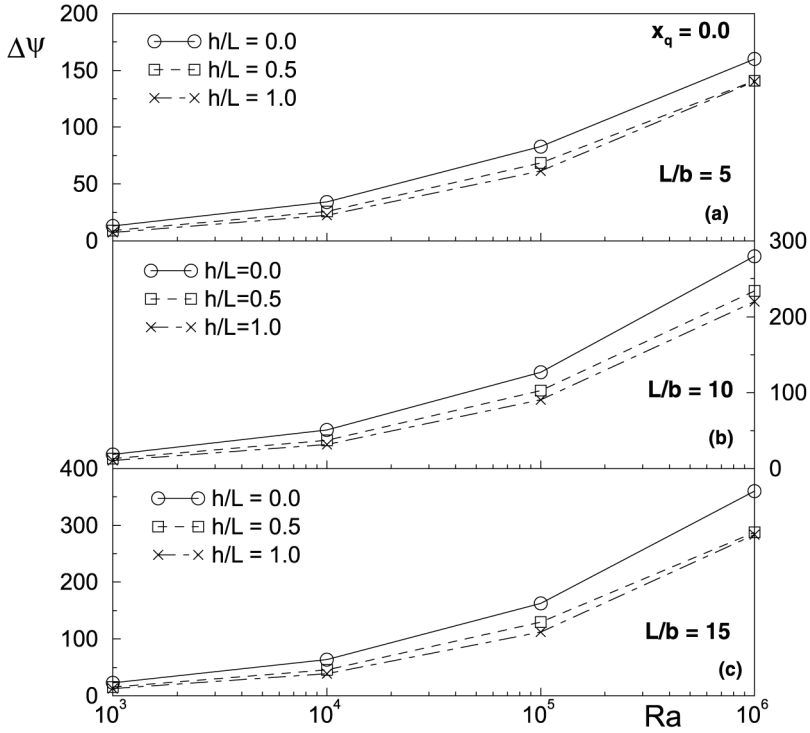

Figure 5.
Dimensionless mass flow rate vs Rayleigh number for different h/L and L/b and $x_q = 0.0$

slightly lower mass flow rate values than in the simple channel. The contrary occurs in the range 10^4–10^5 of the Rayleigh number; its value corresponding to the reversal increases at increasing values of L/b. This indicates that optimal configurations can be found for $\Delta\Psi$ values with reference to the geometric parameter h/L.

Average Nusselt number as a function of the Rayleigh number for the configurations with $L/b = 5$, 10 and 15 and $h/L = 0.0$, 0.5 and 1.0 is shown in Figures 7 and 8, for $x_q = 0.0$ and 1.0, respectively.

Figures 7 and 8 show that the Nusselt number increases as Ra increases both for $x_q = 0.0$ and $x_q = 1.0$, in agreement with the mass flow rate behavior. The average Nusselt number decreases when L/b increases, Ra being constant. Moreover, at the lower Ra values ($\leq 10^4$), Nu decreases when h/L increases, while, at the higher Ra values ($\geq 10^5$), Nu increases when h/L increases. It is worth noticing that the dependence of the Nusselt number on the process parameters is less marked when the auxiliary plate is heated. The Rayleigh number at which the change in the trend occurs is larger at larger aspect ratio values.

The ratio of the dimensionless mass flow rate to the simple channel dimensionless mass flow rate and the ratio of the average Nusselt number to

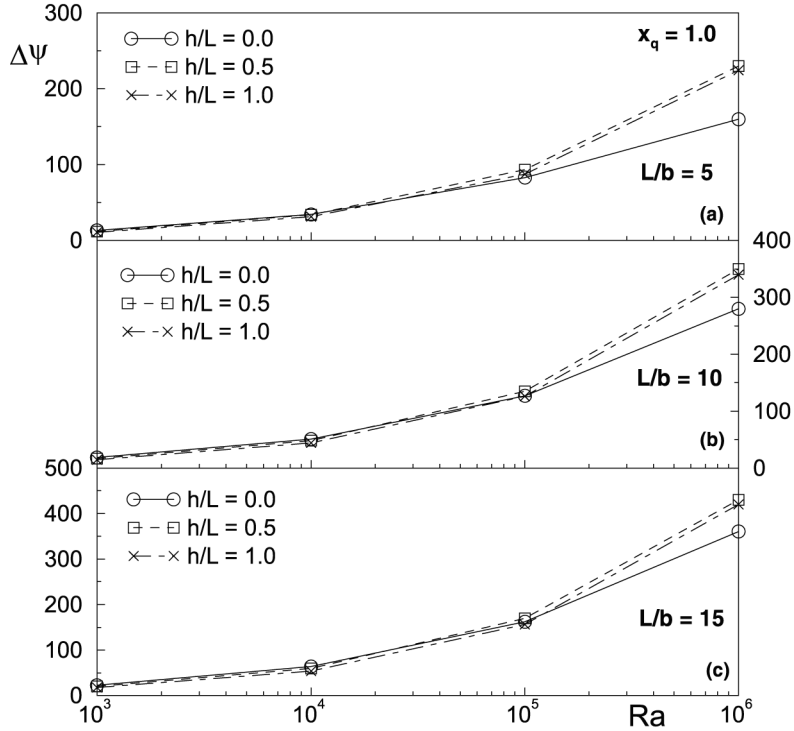

Figure 6.
Dimensionless mass flow rate vs Rayleigh number for different h/L and L/b and $x_q = 1.0$

the simple channel average Nusselt number as a function of h/L, for Ra in the range 10^3–10^6 and for $L/b = 10$, are shown in Figures 9 and 10, for $x_q = 0.0$ and 1.0, respectively.

It can be observed that at all Ra the larger h/L the smaller the mass flow rate. This is due to the increase in the pressure drop when h/L increases. For a fixed h/L, the $\Delta\Psi/\Delta\Psi_0$ ratio increases as the Rayleigh number increases since the larger Rayleigh number the thinner the boundary layer and, consequently, the stronger the chimney effect. At the lower Rayleigh number ($\leq 10^4$), Nu/Nu_0 decreases as h/L increases, while, for $Ra \geq 10^5$, it first increases and then decreases as a function of h/L. Moreover, there is a maximum value close to $h/L = 0.5$, which represents a thermal optimum for the configuration. For $x_q = 1.0$ Figure 10 shows that the dimensionless mass flow rate attains a maximum equal to 1.25, corresponding to an increase equal to about 25 percent that in a simple channel for $Ra = 10^6$ and a maximum equal to 1.05 with a nearly 5 percent increase for $Ra = 10^5$. The maximum values are attained at nearly $h/L = 0.5$ for the analyzed configurations. The average Nusselt number increases for $Ra = 10^5$ and $Ra = 10^6$, and the increase being not larger than 6 percent.

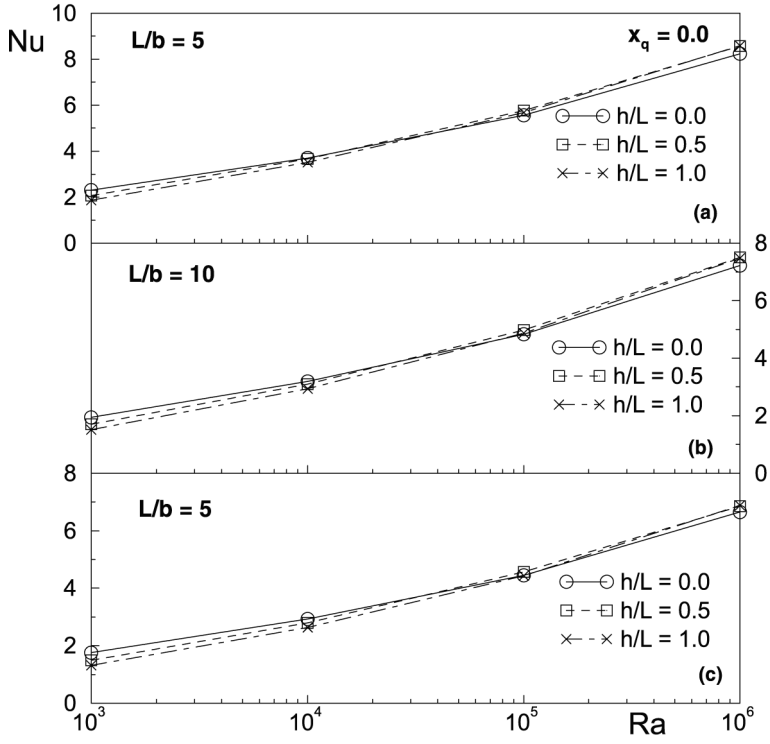

Figure 7.
Average Nusselt number vs Rayleigh number for different h/L and L/b and $x_q = 0.0$

Correlations

Simple monomial correlations are proposed in the following for the dimensionless mass flow rate, $\Delta\Psi$, the dimensionless maximum wall temperature, $\theta_{w1,\max}$ and the average Nusselt number. They are given in terms of the Rayleigh number, Ra, the aspect ratio L/b and the height ratio, h/L, for $x_q = 0.0$ and $x_q = 1.0$. Correlations are a useful tool for the thermal design in many applications, such as thermal control of electronic systems and components. They help to define optimal configurations in terms of both maximum wall temperatures and Nusselt numbers.

For the channel with the unheated auxiliary plate ($x_p = 0.0$), the correlation for the dimensionless mass flow rate is

$$\Delta\Psi = 0.390\left(\mathrm{Ra}\frac{L}{b}\right)^{0.413}\left(1+\frac{h}{L}\right)^{-0.565} \tag{15}$$

with the regression coefficient $r^2 = 0.988$, in the ranges: $10^3 \le \mathrm{Ra} \le 10^6$, $5 \le L/b \le 15$ and $0 \le h/L \le 1$.

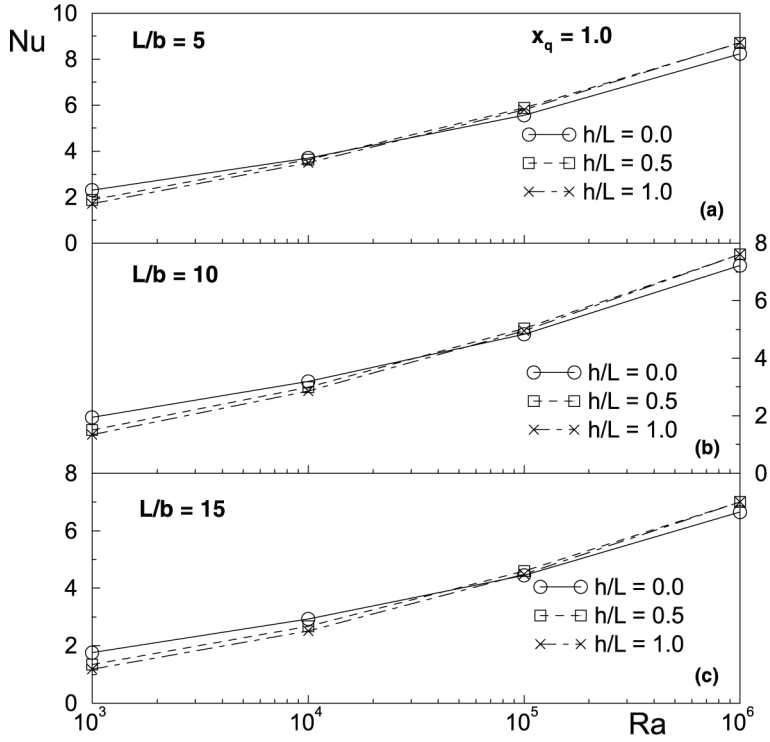

Figure 8.
Average Nusselt number vs Rayleigh number for different h/L and L/b and $x_q = 1.0$

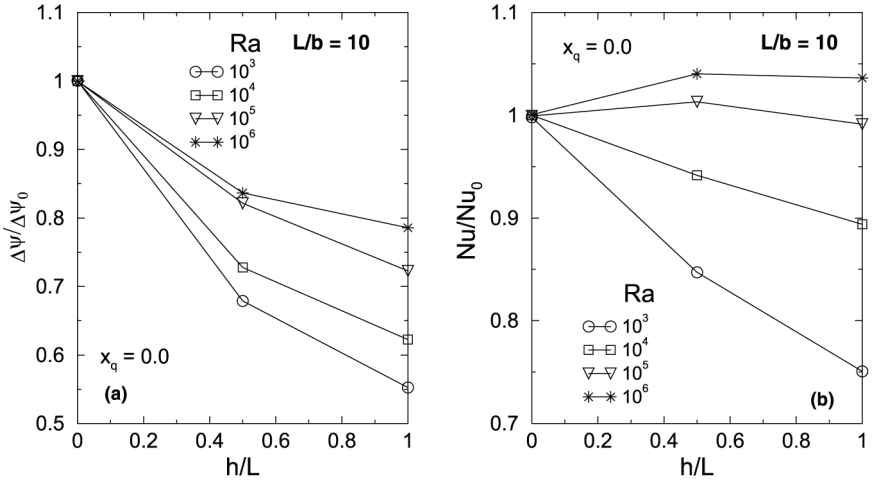

Figure 9.
Ratio of the dimensionless mass flow rate to simple channel one (a) and ratio of the average Nusselt number to simple channel one (b) vs h/L at different Ra for $x_q = 0.0$ and $L/b = 10$

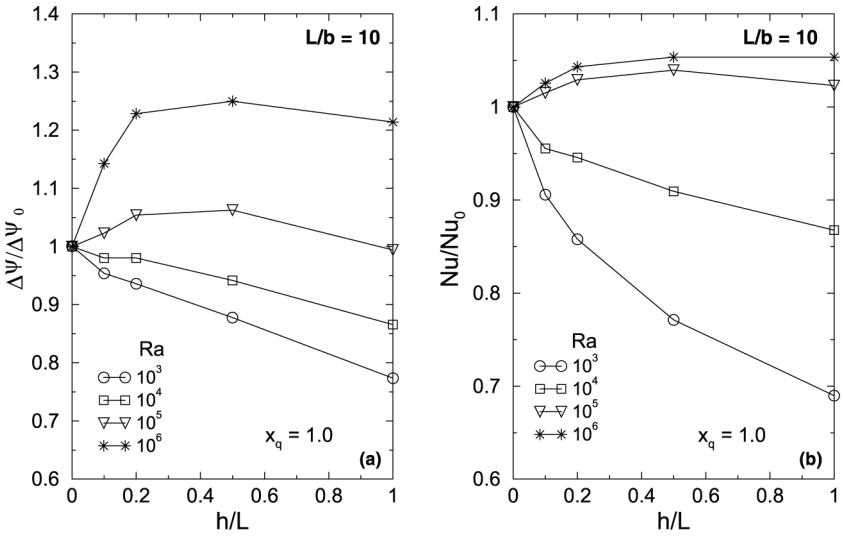

Figure 10.
Ratio of the dimensionless mass flow rate to simple channel one (a) and ratio of the average Nusselt number to simple channel one (b) vs h/L at different Ra for $x_q = 1.0$ and $L/b = 10$

The correlation for the dimensionless maximum wall temperature is

$$\theta_{w1,\max} = 3.60\left(\mathrm{Ra}\frac{L}{b}\right)^{-0.273}\left(1+\frac{h}{L}\right)^{0.246} \tag{16}$$

with $r^2 = 0.979$, in the ranges: $10^3 \le \mathrm{Ra} \le 10^6$, $5 \le L/b \le 15$ and $0 \le h/L \le 1$.

The correlation for the average Nusselt number is

$$\mathrm{Nu} = 0.706\left(\mathrm{Ra}\frac{L}{b}\right)^{0.211}\left(1+\frac{h}{L}\right)^{-0.100} \tag{17}$$

with $r^2 = 0.985$, in the ranges: $10^3 \le \mathrm{Ra} \le 10^6$, $5 \le L/b \le 15$ and $0 \le h/L \le 1$.

For the channel with the heated auxiliary plate ($x_q = 1.0$), the correlation for the dimensionless mass flow rate is

$$\Delta\Psi = 0.350\left(\mathrm{Ra}\frac{L}{b}\right)^{0.426}\left(1+\frac{h}{L}\right)^{-0.0684} \tag{18}$$

with $r^2 = 0.991$, in the ranges: $10^3 \le \mathrm{Ra} \le 10^6$, $5 \le L/b \le 15$ and $0 \le h/L \le 1$.

The correlation for the dimensionless maximum wall temperature is

$$\theta_{w1,\max} = 4.19\left(\mathrm{Ra}\frac{L}{b}\right)^{-0.290}\left(1+\frac{h}{L}\right)^{0.455} \tag{19}$$

with $r^2 = 0.969$, in the ranges: $10^3 \leq \mathrm{Ra} \leq 10^6$, $5 \leq L/b \leq 15$ and $0 \leq h/L \leq 1$.

The correlation for the average Nusselt number is

$$\mathrm{Nu} = 0.639\left(\mathrm{Ra}\frac{L}{b}\right)^{0.223}\left(1+\frac{h}{L}\right)^{-0.140} \tag{20}$$

with $r^2 = 0.976$, in the ranges: $10^3 \leq \mathrm{Ra} \leq 10^6$, $5 \leq L/b \leq 15$ and $0 \leq h/L \leq 1$. It can be observed that the coefficients in the correlations for the average Nusselt number are very similar to those in the correlation for the simple channel with uniform heat flux at the walls (Bar-Cohen and Rohsenow, 1984).

Conclusions

The influence of the fundamental thermo-geometrical parameters on the thermal performance of a channel with an auxiliary plate placed in its mid-plane has been numerically investigated. The formulation in terms of stream function–vorticity ($\Psi-\Omega$) has been employed to solve the Navier–Stokes equations. The numerical solution has been carried out using the finite control volume approach on a computational domain with a lower and an upper reservoir. The investigation has been accomplished for a Prandtl number of 0.71. The auxiliary plate worsens the local heat transfer rate, particularly at the lowest Rayleigh number under investigation (10^3). This occurs at all analyzed L/b values and it increases as h/L increases when the auxiliary plate is both heated and unheated. When the auxiliary plate is not heated the larger h/L the smaller the mass flow rate and the larger L/b the larger the decrease in the mass flow rate. For the configuration with the heated auxiliary plate, increasing the Rayleigh number increases the mass flow rate. The reversal of trend depends on L/b; in fact, the Ra value corresponding to the reversal increases as L/b increases. The heat transfer, in terms of the average Nusselt number, improves at the higher Ra for all the investigated configurations with the auxiliary plate with respect to the simple channel. Optimal configurations in terms of average channel Nusselt numbers are obtained for $\mathrm{Ra} \geq 10^5$ and for both $x_q = 0.0$ and $x_q = 1.0$. The increase is not larger than 6 percent and it is obtained for h/L at about 0.5. Correlations in a very simple form are proposed in the ranges: $10^3 \leq \mathrm{Ra} \leq 10^6$, $5 \leq L/b \leq 15$ and $0 \leq h/L \leq 1$. It is interesting to observe that coefficients in the correlations for average channel Nusselt number are very close to those in the correlation for simple channel with uniform wall heat flux given in the literature.

References

Andreozzi, A. and Manca, O. (2001), "Thermal and fluid dynamic behaviour of symmetrically heated vertical channels with auxiliary plate", *International Journal of Heat and Fluid Flow*, Vol. 22, pp. 424-32.

Andreozzi, A., Campo, A. and Manca, O. (2000), "Aggregate intensification of natural convection between air and a vertical parallel-plate channel by inserting an auxiliary plate at the mouth and appending collinear insulated plates at the exit", in ASME-HTD, Orlando, Florida, USA Vol. 366-4, pp. 421-6.

Andreozzi, A., Manca, O. and Morrone, B. (1999), "Numerical analysis of natural convection in symmetrically heated vertical channels with an auxiliary parallel plate", in NHTC-HTD/117, Albuquerque, New Mexico, USA.

Aihara, T., Ohara, T., Sasago, A., Ukaku, M. and Gori, F. (1996), *Augmentation of Free-Convection Heat Transfer between Vertical parallel Plates by Inserting and Auxiliary Plate*, 2nd European Thermal Sciences, Rome, Italy.

Bar-Cohen, A. and Kraus, A.D. (1998), *Advances in Thermal Modeling of Electronic Components and Systems*, Hemisphere Publ. Co., ASME Press, New York, USA, Vol. 4.

Bar-Cohen, A. and Rohsenow, W.M. (1984), "Thermally optimum spacing of vertical natural convection cooled, parallel plates", *ASME Journal of Heat Transfer*, Vol. 106, pp. 116-23.

Bejan, A. (1984), *Convection Heat Transfer*, Wiley, New York, USA.

Bianco, N., Morrone, B., Nardini, S. and Naso, V. (2000), "Air natural convection between inclined parallel plates with uniform heat flux at the walls", *Journal of Heat and Technology*, Vol. 18 No. 2, pp. 23-45.

Cheng, C.H., Huang, W.H. and Kou, H.S. (1988), "Laminar free convection of the mixing flows in vertical channels", *Numerical Heat Transfer, Part A*, Vol. 14, pp. 447-63.

Floryan, J.M. and Novak, M. (1994), "Free convection heat transfer in multiple vertical channels", *International Journal of Heat and Fluid Flow*, Vol. 16, pp. 244-53.

Gebhart, B., Jaluria, Y., Mahajan, R. and Sammakia, B. (1988), *Buoyancy-Induced Flows and Transport*, Hemisphere Publ. Corp., Washington, D.C.

Kim, S.J. and Lee, S.W. (1996), *Air Cooling Technology for Electronic Equipment*, CRC Press, Boca Raton, Fl.

Ledezma, G.A. and Bejan, A. (1997), "Optimal geometric arrangement of staggered vertical plates in natural convection", *ASME Journal of Heat Transfer*, Vol. 119, pp. 700-8.

Manca, O. and Nardini, S. (2001), "Thermal design of uniformly heated inclined channels in natural convection with and without radiative effects", *Heat Transfer Engineering*, Vol. 22, pp. 13-28.

Manca, O., Morrone, B. and Naso, V. (1994), "A numerical study of natural convection between symmetrically heated vertical parallel plates", *Atti del XII Congresso Nazionale sulia Transmissione del Calore, L'Aquila*, Italy pp. 379-90.

Manca, O., Morrone, B., Nardini, S. and Naso, V. (2000), "Natural convection in open channels", in Sundén, B., Comini, G. (Eds), *Computational Analysis of Convection Heat Transfer*, WIT Press, Southampton, Boston pp. 236 -78.

Morrone, B., Campo, A. and Manca, O. (1997), "Optimum plate separation in a vertical parallel-plate channel for natural convection flows: incorporation of large spaces at the channel extremes", *International Journal of Heat and Mass Transfer*, Vol. 40, pp. 993-1000.

Naylor, D. and Tarasuk, J.D. (1993a), "Natural convective heat transfer in a divided vertical channel: part 1.: Numerical study", *ASME Journal of Heat Transfer*, Vol. 115, pp. 377-87.

Naylor, D. and Tarasuk, J.D. (1993b), "Natural convective heart transfer in a divided vertical channel: part 2: experimental study", *ASME Journal of Heat Transfer*, Vol. 115, pp. 388-99.

Peterson, G.P. and Ortega, A. (1990), "Thermal control of electronic equipments and devices", *Advances in Heat Transfer*, Vol. 20, pp. 181-314.

Raithby, G.D. and Hollands, K.G.T. (1998), *Handbook of Heat Transfer*, chapter 4, 3rd edition, McGraw-Hill, New York.

Roache, J.P. (1998), *Verification and Validation in Computational Science and Engineering*, Hermosa publ., Albuquerque, NM.